

### 3.6 A Kelvin Bore.

A type of shock that can be treated with some success is the bore formed by a Kelvin wave propagating into a quiescent region of uniform depth. Examples arise in the nonlinear version of the Rossby adjustment problem when the channel is wider than several deformation radii. The downstream bore then consists of an abrupt change in depth that is trapped to the right channel wall (Figure 3.3.6). The near discontinuity in depth is aligned perpendicular to the wall at the contact point but is increasingly oblique away from the wall. In contrast with the bore observed in narrower channels (e.g. Figure 3.3.7) the present feature is felt only weakly at the left wall. The lack of influence of the left wall was exploited by Federov and Melville (1996) who developed a model describing the shape and speed of the bore.

Suppose that the discontinuity lies along a contour  $y=Y(x,t)$  (Figure 3.6.1). It will be assumed that  $w$  is infinite so that the left wall is removed entirely. The fluid lying ahead ( $y>Y$ ) is quiescent and the fluid lying immediately behind has velocity  $u=u_o(x,t)$ ,  $v=v_o(x,t)$ , and depth  $d=1+a(x,t)$ . If the continuity equation (2.1.7) is integrated over a fixed interval  $y_1 \leq y \leq y_2$  containing the shock, and if the interval is then reduced to zero, it follows that

$$\int_{y_1}^{y_2} \frac{\partial d}{\partial t} dy + \int_{y_1}^{y_2} \frac{\partial(ud)}{\partial x} dy - v_o(1+a) = 0. \quad (3.6.1)$$

Since the integration interval is fixed, the derivatives may be taken outside of the integral and therefore

$$\int_{y_1}^{y_2} \frac{\partial d}{\partial t} dy = \frac{\partial}{\partial t} \int_{y_1}^{y_2} (d) dy = \frac{\partial}{\partial t} \left[ \int_{y_1}^Y (d) dy + \int_Y^{y_2} (d) dy \right] = \frac{\partial Y}{\partial t} [(1+a) - 1] = a \frac{\partial Y}{\partial t}$$

After a similar treatment of its second term and division by  $(1+a)$ , (3.6.1) becomes

$$\frac{a}{1+a} \frac{\partial Y}{\partial t} + u_o \frac{\partial Y}{\partial x} - v_o = 0 \quad (3.6.2)$$

A second constraint follows from the continuity of the tangential velocity across the discontinuity (see 3.5.4). Since the fluid ahead of the discontinuity is quiescent the tangential velocity to the rear must also be zero:

$$v_o \frac{\partial Y}{\partial x} + u_o = 0 \quad (3.6.3)$$

A third constraint results from integration across the discontinuity of the flux form (2.1.17a) of the y-momentum equation. The resulting condition is

$$v_o \frac{\partial Y}{\partial t} - \left( v_o^2 + \frac{a(1 + \frac{1}{2}a)}{(1+a)} \right) + u_o v_o \frac{\partial Y}{\partial x} = 0 \quad (3.6.4)$$

Using (3.6.3) to eliminate  $u_o$  from (3.6.2) and (3.6.4) leads to

$$\frac{a}{1+a} \frac{\partial Y}{\partial t} = v_o \left[ 1 + \left( \frac{\partial Y}{\partial x} \right)^2 \right] \quad (3.6.5)$$

and

$$v_o \frac{\partial Y}{\partial t} - \frac{a(1 + \frac{1}{2}a)}{(1+a)} = v_o^2 \left[ 1 + \left( \frac{\partial Y}{\partial x} \right)^2 \right]. \quad (3.6.6)$$

Eliminating  $\partial Y / \partial x$  between the last two equations gives

$$v_o = \frac{a(1 + \frac{1}{2}a)}{\partial Y / \partial t} \quad (3.6.7)$$

and substitution for  $v_o$  back into (3.6.5) yields

$$\left( \frac{\partial Y}{\partial t} \right)^2 = (1+a)(1 + \frac{1}{2}a) \left[ 1 + \left( \frac{\partial Y}{\partial x} \right)^2 \right]. \quad (3.6.8)$$

Now suppose that the discontinuity propagates along the wall at a steady speed  $\partial Y / \partial t = c$ , so that

$$\begin{aligned} c^2 &= (1+a)(1 + \frac{1}{2}a) \left[ 1 + \left( \frac{\partial Y}{\partial x} \right)^2 \right] \\ &= \frac{(1+a)(1 + \frac{1}{2}a)}{\cos^2 \theta}, \end{aligned} \quad (3.6.9)$$

where  $\theta$  is the angle between the line of discontinuity and the normal to the wall.  $\partial Y / \partial x$  must vanish at the point of contact in order to satisfy the condition of no normal flow, and it follows that

$$c^2 = (1+a_o)(1 + \frac{1}{2}a_o) \quad (3.6.10)$$

where  $a_o$  is the value of  $a$  at the wall. This  $c$  is equivalent to the speed of a non-rotating, one-dimensional bore propagating into shallow water (see equation 1.6.7 with  $v_u=0$ ), based on the wall depth. Equation (3.6.9) can now be written as

$$\left( \frac{\partial Y}{\partial x} \right)^2 = \frac{(1+a_o)(1 + \frac{1}{2}a_o)}{(1+a)(1 + \frac{1}{2}a)} - 1. \quad (3.6.11)$$

The factor  $(1+a)(1+\frac{1}{2}a)$  appearing in the last few equations can now be seen to have a simple interpretation. Consider a small segment of the discontinuity that is aligned at an angle  $\theta$  and therefore faces the direction  $(-\sin\theta, \cos\theta)$ , as shown in the Figure 3.6.1 inset. Since the entire bore translates at speed  $c = [(1+a)(1+\frac{1}{2}a)]^{1/2} / \cos(\theta)$ , the segment in question moves in the  $y$ -direction at this speed. The speed of the front in the normal direction is therefore  $[(1+a)(1+\frac{1}{2}a)]^{1/2}$ . Equation (3.6.9) is just a statement of this geometrical consideration. At the wall, where  $y$  is the normal direction,  $c$  is given by (3.6.10). Since  $c$  is constant, the amplitude  $a$  of the discontinuity must diminish as  $\theta$  increases.

A solution for  $Y$  as a function of  $x$  cannot be ascertained without a further assumption about the flow to the rear of the jump. Federov and Melville (1996) take the velocity component  $v_o$  to be geostrophic:

$$v_o = \frac{\partial a}{\partial x}, \quad (3.6.12)$$

implying that the non-semigeostrophic region  $R$  described in the previous section is absent. This approximation is justified as long as the transverse velocity  $u_o$  remains  $\ll v_o$ , and this requires that the angle  $\theta$  between the discontinuity and the  $x$ -axis remains small (cf. equation 3.6.3).

Substitution of (3.6.12) into (3.6.7) leads to

$$\frac{da}{dx} = \frac{a(1+\frac{1}{2}a)}{c}.$$

If the right wall is temporarily assumed to lie at  $x=0$ , the solution satisfying  $a(0)=a_o$  is given by

$$a(x) = \frac{a_o e^{x/c}}{1 + \frac{1}{2}a_o(1 - e^{x/c})}. \quad (3.6.13)$$

Far from the wall ( $x \rightarrow -\infty$ )  $a \rightarrow 0$  and, according to (3.6.11),

$$\left(\frac{\partial Y}{\partial x}\right)_{\infty}^2 = \tan^2(\theta_{\infty}) = \frac{1}{2}a_o(3 + a_o).$$

The far field angle  $\theta_{\infty}$  between the jump and the  $x$ -axis tends to zero as the amplitude  $a_o$  is reduced. When  $a_o$  reaches 0.56,  $\theta_{\infty}$  is  $45^\circ$ .

The shape of the contour  $y=Y$  can be found by substituting (3.6.13) into (3.6.11) and integrating that relation numerically. Examples of solutions for various  $a_0$  (Figure 3.6.2) show the curvature previously alluded to. The curvature and the angle  $\theta$  increase as  $a_0$  does but Federov and Melville (1996) show that the geostrophic approximation for  $v_0$  remains good as long as  $a_0 < 1$ .

The above theory does not allow for the presence of a left channel wall. In the simulations carried out by Helfrich et al. (1999), Poincaré wave radiation is observed where the bore contacts the left wall (e.g. Figure 3.3.7). The presence of such waves requires a non-geostrophic  $v$  and thus a violation of (3.6.12). A comparison between the predicted bore speed and the speed measured from simulations by Helfrich et al. (1999) shows that the observed speed is well predicted when the channel is narrow, essentially the non-rotating limit (Figure 3.6.3). As the channel width increases from moderate to large values in comparison with the deformation radius, the observed speed is overpredicted by (3.6.10), perhaps due to the radiation of Poincaré waves.

### Exercises

1. Obtain (3.6.4) through integration of (3.2.3) across the discontinuity and interpretation of the normal and tangential directions ( $n$  and  $s$ ) as  $y$  and  $-x$ .

### Figures

Figure 3.6.1 Definition sketch for a Kelvin wave bore propagating along a coastline.

Figure 3.6.2 Solutions showing the path of the discontinuity  $y=Y(x)$  in the moving frame of the bore for various values  $a_0$ . (Based on Federov and Melville, 1996, Figure 13.)

Figure 3.6.3 Comparison between the speed predicted by (3.6.10) (solid curves) and the speed observed by Helfrich et al. (1999) in their numerical calculations for various finite channel widths [ $w=0$  (O), 0.2 ( ), 0.5 (◇), 1.0(Δ), 2.0(★) and 4.0(Δ)], where  $w$  has been scaled by the Rossby radius based on the depth  $d_d^*$  in the quiescent region ahead of the bore. The bore speed  $c$  has been nondimensionalized by  $(gd_d^*)^{1/2}$  and the bore amplitude  $a$  has been scaled by  $d_d^*$ . (From Helfrich et al. 1999)

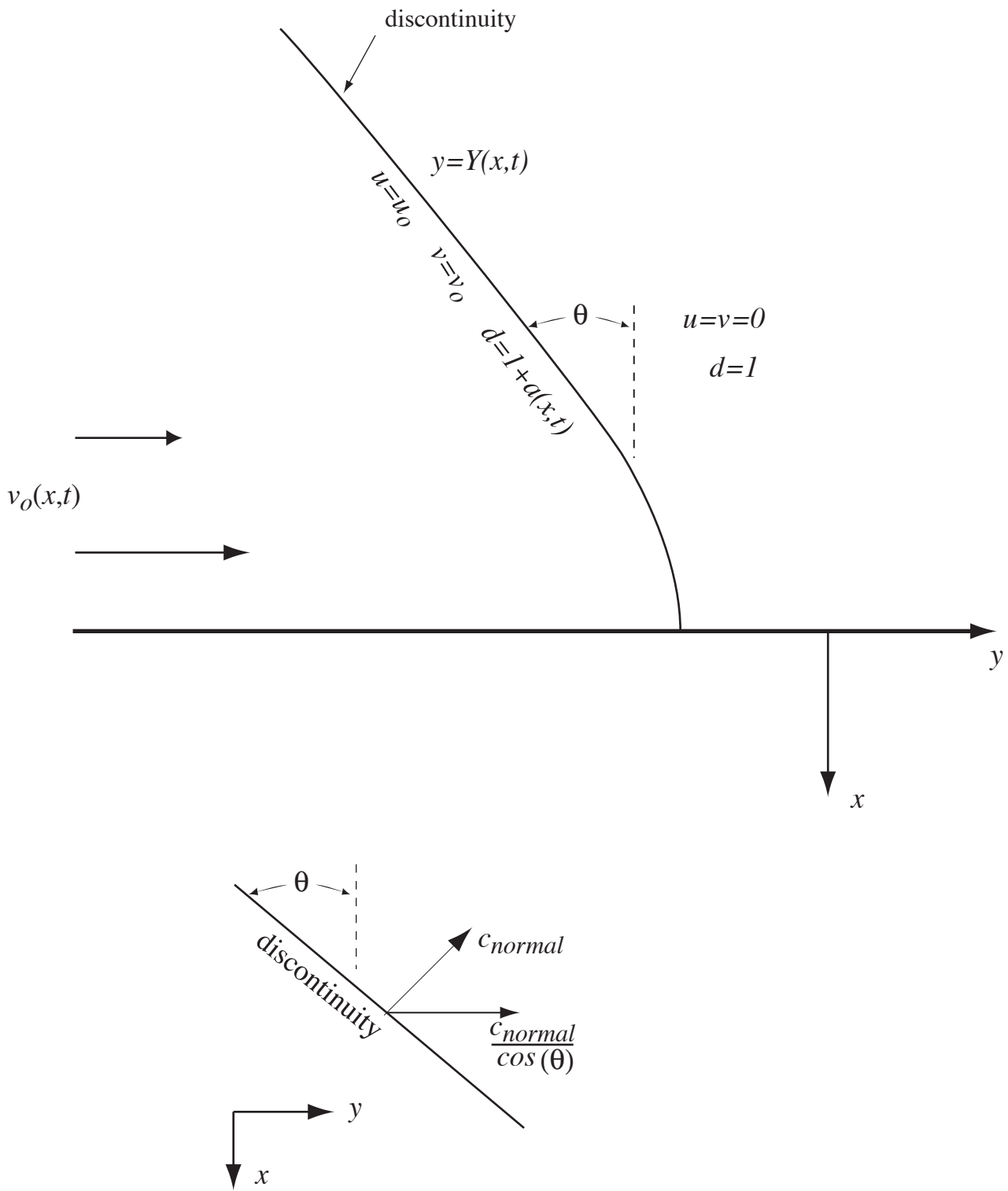


Figure 3.6.1

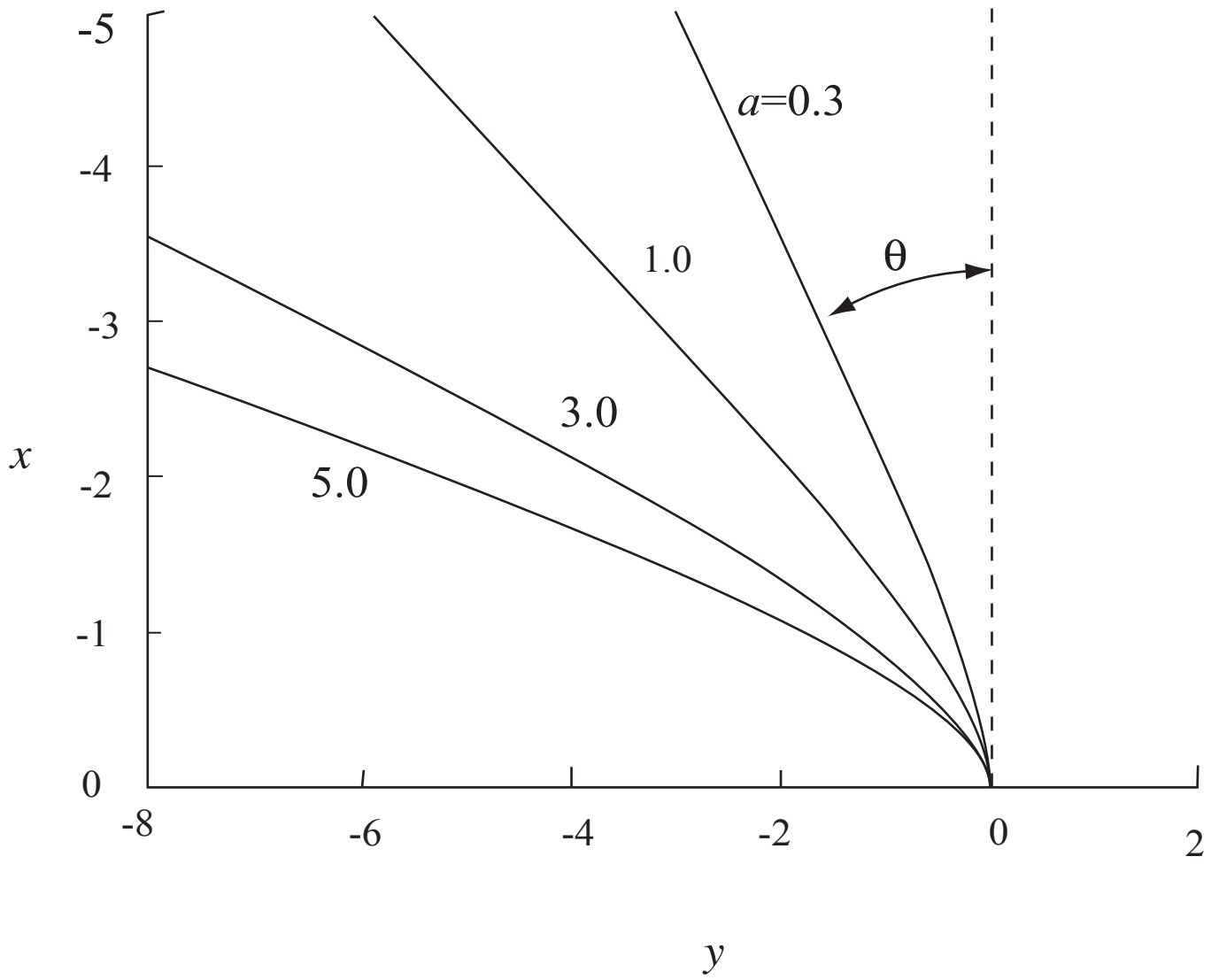


Figure 3.6.2

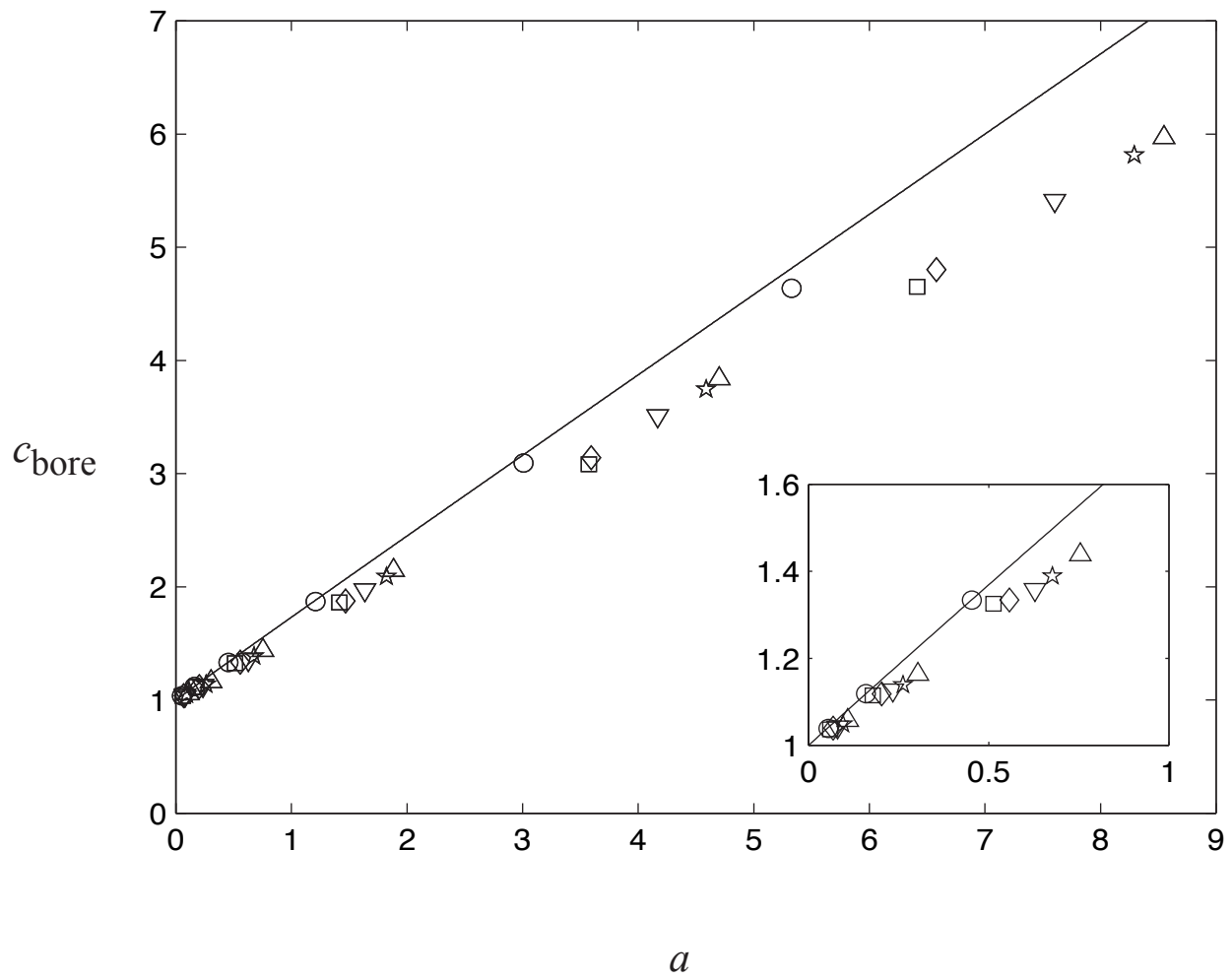


Figure 3.6.3